

The Effectiveness Of Moringa Extract Cream On Collagen Fiber Density In The Wound Healing Process After Incision In White Rats (*Rattus Norvegicus*)

Ariska Putri Pertiwi¹, Tan Suyono², Linda Chiuman^{3*}

¹Department of Master of Biomedical Science, Faculty of Medicine, Dentistry, and Health Sciences, Prima Indonesia University, 20113, Indonesia

*E-mail : lindachiuman@unprimdn.ac.id

ABSTRACT

Moringa (*Moringa oleifera*) leaf extract cream is believed to accelerate wound healing by enhancing collagen fiber density and compactness in skin tissue. This experimental study aimed to evaluate the effectiveness of *Moringa oleifera* leaf extract cream on collagen fiber density during the healing of incision wounds in white rats (*Rattus norvegicus*). Twenty-four male C57BL/6 strain rats were divided into four groups: control (placebo) and treatment groups receiving 5%, 10%, and 15% moringa extract cream. The cream was applied twice daily for 14 days. Wound tissues were then examined histopathologically using Masson's Trichrome staining to assess collagen density. Macroscopic observations showed that the treatment groups, particularly the 15% concentration, exhibited faster wound closure compared to the control. Histologically, the treatment groups demonstrated higher collagen deposition and denser fiber organization. However, one-way ANOVA analysis ($p = 0.791$) indicated no statistically significant differences among groups. Despite the lack of significance, an increasing trend in collagen density was evident in the 10% and 15% treatment groups. These findings suggest that *Moringa oleifera* extract cream may promote wound healing and improve collagen formation, though further studies with larger samples and longer observation periods are needed to confirm its efficacy.

Keywords: *Moringa oleifera*, collagen, wound healing, white rats, herbal cream

INTRODUCTION

A wound is an injury to body tissue caused by various factors such as physical trauma, infection, disease, or medical interventions like surgery. Wounds vary in severity, from minor ones that heal quickly to severe injuries requiring intensive care and long recovery time. They can also be classified based on depth, ranging from superficial wounds that affect only the outer skin layer to deeper wounds that damage underlying tissues, including muscles, nerves, and blood vessels (Kamal, 2019: 22). Wound healing is a complex and coordinated biological process aimed at restoring the integrity of damaged tissue. It consists of three main phases: inflammation, proliferation, and remodeling—each playing a vital role in ensuring effective healing and preventing complications such as infection or excessive scarring. During the inflammatory phase, which occurs immediately after injury, nearby blood vessels undergo vasoconstriction to reduce bleeding, followed by vasodilation to increase blood flow to the injured area. This blood flow brings immune cells such as neutrophils and macrophages, which

help remove pathogens and debris and release cytokines and growth factors that trigger subsequent healing stages (Kartika, 2024: 28). The proliferation phase, lasting from several days to weeks, involves epithelial cell migration to cover the wound and fibroblast activity that produces collagen to form new granulation tissue. Collagen plays a crucial role in providing strength and structure to newly formed tissue. This stage also involves angiogenesis, the formation of new blood vessels that supply oxygen and nutrients needed for recovery (Primadina, Basori, & Perdanakusuma, 2019: 11). The final stage, remodeling, strengthens and reorganizes the new tissue. Excess collagen is degraded, and the remaining collagen fibers are realigned to provide maximum tensile strength. This phase can take months to years, depending on wound type and depth (Mardiyantoro, 2022: 21).

Moringa oleifera, commonly known as moringa, is a plant renowned for its rich nutritional content and various health benefits. Studies have shown that moringa extract has anti-inflammatory, antioxidant, and cell-regenerative properties—all essential in wound healing. Its bioactive compounds, such as flavonoids, polyphenols, and vitamin C, are believed to accelerate healing. Flavonoids and polyphenols act as antioxidants that fight free radicals and reduce inflammation, while vitamin C supports collagen synthesis, a key structural component in tissue repair. By enhancing collagen production, moringa may help accelerate new tissue formation and reduce excessive scar formation. Therefore, moringa extract, particularly in topical form such as moringa cream, shows great potential as a woundhealing agent (Asrul, Rivai, Syisnawati, & Haristiani, 2023: 10).

White rats are frequently used as biomedical research models, including in woundhealing studies, for several important reasons. First, they share significant genetic similarities with humans, making experimental results more translatable. Second, their short life cycle allows researchers to observe therapeutic effects in a relatively short period. Additionally, they are easy to maintain and cost-effective, making them ideal for large-scale laboratory studies. These factors make white rats an efficient and practical model for studying complex biological processes such as wound healing (Aria, Fendri, & Muqaddar, 2022: 7). Based on this background, further research is needed to determine whether moringa extract cream can enhance collagen fiber density and accelerate the healing of incision wounds in white rats.

The main objective of this study is to determine the effectiveness of *Moringa oleifera* extract cream in increasing collagen fiber density during the healing process of incision wounds in white rats (*Rattus norvegicus*). This research was conducted based on the need to explore natural and affordable alternatives that can enhance wound recovery and tissue regeneration. The motivation behind this study arises from the potential of *Moringa oleifera*, which is known to contain bioactive compounds such as flavonoids, polyphenols, and vitamin C that play important roles in collagen synthesis and tissue repair. To achieve this, the study aims to analyze the effect of moringa extract cream on wound healing speed, compare collagen fiber density between treated and control groups, identify the most effective concentration of moringa extract cream, and examine its phytochemical content. Through an experimental design using white rats, this research seeks to contribute to the development of topical herbal formulations that may support faster and stronger wound healing. The findings are expected to provide valuable insights for biomedical research and natural product development in the field of tissue repair and recovery.

METHODS

This study employed an experimental research design, which is a method aimed at testing hypotheses by controlling and manipulating independent variables to observe their effects on dependent variables while maintaining control over other factors. In this approach, the researcher actively manages the conditions and treatments received by the subjects—in this case, white rats—to establish a causal relationship between variables. This method provides stronger and more valid evidence of the effects of a particular treatment compared to observational or descriptive studies (Jaedun, 2021: 14). The experimental design was chosen because it allows direct manipulation of the independent variable, namely the administration of *Moringa oleifera* extract cream, and direct measurement of its influence on the dependent variable, collagen fiber density, thus enabling a clearer understanding of cause-and-effect relationships.

The study was conducted in May 2025 at the Laboratory of the University of North Sumatra, selected for its adequate facilities and equipment for animal testing. The independent variable was the administration of *Moringa oleifera* extract cream with varying doses and frequencies—5%, 10%, and 15% concentrations—applied twice daily for two weeks, while the control group received only a placebo cream (Indriyana, 2023: 10; Wahyuningrum & Probosari, 2022: 9). The dependent variable, collagen fiber density, was measured using histopathological methods through Masson’s Trichrome staining to count collagen fibers per unit area in the wound tissue, allowing accurate visualization and comparison between treatment groups (Duarsa, 2020: 12; Nanda, Salim, & Iskandar, 2022: 11).

Controlled variables included the sex of the rats—all male to minimize hormonal variations (Zilmi, 2021: 8); age—uniformly 8–10 weeks to ensure physiological consistency (Listiani, 2021: 7); strain—C57BL/6 for genetic uniformity (Siagian & Christyaningsih, 2023: 16); wound size—standardized to 2–3 cm for comparable tissue injury (Erwiyani, Haswan, Agasi, & Karminingtyas, 2020: 13); and experimental duration—fixed at 14 days to ensure consistent exposure time across groups (Sandyarani, 2022: 18). **Table 1. Control Variables**

Control Variable	Description
Sex of White Rats	All white rats were male to avoid hormonal variability (Zilmi, 2021: 8).
Age of White Rats	The rats were 8–10 weeks old to ensure consistent physiological responses (Listiani, 2021: 7).
Strain of White Rats	All rats were of the C57BL/6 strain to minimize genetic variability (Siagian & Christyaningsih, 2023: 16).
Wound Size	The wound size was standardized at 2–3 cm to ensure equal tissue injury across groups (Erwiyani et al., 2020: 13).
Experiment Duration	The duration of the experiment was set to 14 days to maintain result consistency (Sandyarani, 2022: 18).

An operational definition explains how research variables are measured concretely in the field (Listiani, 2021: 9). In this study, there are three main variables: the administration of *Moringa oleifera* extract cream, collagen fiber density, and wound healing time. Each variable was clearly defined and measured to ensure accuracy and consistency in data collection. The administration of *Moringa* extract cream refers to the topical application of cream with specific concentrations and frequencies to observe its effect on wound healing. Collagen fiber density

represents the number of collagen fibers per unit area in the wound tissue, measured through histopathological examination using Masson's Trichrome staining. Meanwhile, wound healing time refers to the duration required for the wound to close completely, assessed visually each day until full closure was observed. The operational details and measurement methods of these variables are summarized in the following table (Utoyo, 2022: 12).

Table 2. Operational Definitions

Variable	Operational Definition	Method	Measurement Tool
Administration of Moringa Extract Cream	Application of <i>Moringa oleifera</i> extract cream at concentrations of 5%, 10%, and 15%, applied twice daily for 14 days.	Applied topically using a sterile spatula on the wound area; recorded in a daily application log.	Percentage (%) and frequency (times/day)
Collagen Fiber Density	Number of collagen fibers per unit area of wound tissue, measured using Masson's Trichrome staining and microscopic analysis.	Analyzed under a light microscope; average collagen fibers counted in five different visual fields.	Fibers/ μm^2 (quantitative scale)
Wound Healing Time	The time required for complete wound closure, measured in days from day 0 until full closure.	Observed visually and recorded daily; wound considered healed when no exudate remains and wound edges fully merge.	Days (ratio scale)

The tools and materials used in this study included animal cages, microscopes, microscope cameras, surgical instruments, ovens, incubators, analytical balances, wound measuring devices, and various chemicals for preparing fixative solutions, stains, and mounting media (Listiani, 2021: 12). Healthy white rats were selected and treated with Moringa extract cream at concentrations of 5%, 10%, and 15%, along with distilled water and other supporting chemicals for histological preparation (Utoyo, 2022: 14). The experimental procedure began with selecting healthy male rats aged around two months and weighing 20–30 grams. The rats were acclimated for seven days before being randomly divided into four treatment groups: a control group without Moringa extract and three treatment groups receiving 5%, 10%, and 15% concentrations (Krisnawati, 2023: 8). Based on Federer's formula, each group consisted of six rats, making a total of 24 subjects for the experiment.

The incision wounds, measuring about 2–3 cm, were made on the dorsolateral area after light anesthesia. The control group received a placebo cream, while the treatment groups received Moringa extract cream twice daily for 14 days (Puspitasari, 2022: 9). Wound healing was observed daily, and the size of the wound was measured regularly using a ruler or caliper. On the 14th day, the rats were ethically euthanized, and skin tissues from the wound areas were collected for histopathological analysis (Furadantin, 2022: 11). The tissue samples were processed through fixation in 10% formalin, dehydration, clearing, paraffin embedding, sectioning with a microtome, staining using Masson's trichrome, and mounting for microscopic examination (Woldemichael, 2022: 17). Collagen fiber density was then counted in five random microscopic fields per sample (Cania & Setyaningrum, 2023: 18).

The Moringa extract cream was prepared using 100 grams of fresh Moringa leaves, macerated in 70% ethanol for three days, filtered, and evaporated to obtain a thick extract (Krisnawati,

2023: 10). The extract was then mixed with a cream base containing emulsifying ointment and aquadest to reach concentrations of 5%, 10%, and 15% (Puspitasari, 2022: 7). During preparation, the base cream was maintained at 60–70°C to melt the emulsifier and oil, then cooled to 40–45°C before adding the Moringa extract. This temperature control was essential to preserve bioactive compounds such as flavonoids, tannins, and vitamin C that play crucial roles in accelerating wound healing (Triastuti, Putri, & Hasya, 2023: 13; CedilloCortezano, Martinez-Cuevas, & Gonzalez, 2024: 15). The cream mixture was stirred until homogeneous and cooled before being stored in sterile containers (Safta, Bogdan, & Moldovan, 2022: 16).

Data analysis included descriptive analysis to present findings in tables and graphs showing sample characteristics and wound healing results (Zellatifanny & Mudjiyanto, 2022: 19). Inferential statistics, such as ANOVA and t-tests, were applied to determine significant differences between the control and treatment groups (Furadantin, 2022: 20). When significant differences were found, post hoc tests were used to identify which specific groups differed in collagen fiber density and healing time (Cania & Setyaningrum, 2023: 18).

RESULTS

Description of Research Results

First, a macroscopic observation is performed. On Day 1, the placebo group (Figure 1 and 2: Placebo, Day 1) showed open incision wounds with slight bleeding and mild inflammation. After applying the placebo cream, only surface moisture appeared, indicating that the cream acted merely as a physical barrier without active healing effects.



Figure 5. Placebo Cream Before Application (Day 1)

Before applying the placebo cream, the incision wound appeared open with slight bleeding and local inflammation, showing that healing had not yet started.



Figure 2. Placebo Cream After Application (Day 1)

After application, no visible improvement was observed except for mild surface moisture, indicating the placebo acted only as a protective barrier.



Figure 3. Before Applying Moringa 5% Cream (Day 1)

Before treatment, the wound condition resembled the placebo group, with visible incision lines and minimal clotting.



Figure 4. After Applying Moringa 5% Cream (Day 1)

After application, a thin protective layer appeared, helping to maintain wound moisture and support early inflammatory processes.



Figure 5. Before Applying Moringa 10% Cream (Day 1)

The incision was still open and clear, showing no natural closure prior to treatment.



Figure 6. After Applying Moringa 10% Cream (Day 1)

A thicker coating of cream covered the wound, helping retain moisture and stimulating early cellular repair activity.



Figure 7. Before Applying Moringa 15% Cream (Day 1)

The wound appeared deep and sharply bordered, indicating fresh tissue damage.



Figure 8. After Applying Moringa 15% Cream (Day 1)

After application, the surface became evenly covered, suggesting that a higher dose provided better local stability for healing initiation.



Figure 9. Placebo Cream Before Application (Day 7)

By Day 7, the placebo wound still appeared wide with incomplete tissue contraction and visible scarring.



Figure 10. Placebo Cream After Application (Day 7)

Minimal improvement was seen, and the wound edges remained separated, indicating slow repair progress.



Figure 11. Before Applying Moringa 5% Cream (Day 7)

At 5% concentration, the wound began to narrow slightly with early dry tissue formation.



Figure 12. After Applying Moringa 5% Cream (Day 7)

Granulation tissue appeared more visible, showing moderate progress though healing remained incomplete.



Figure 12. Before Applying Moringa 10% Cream (Day 7)

The wound was smaller than the placebo group and showed early signs of contraction.



Figure 13. After Applying Moringa 10% Cream (Day 7)

A stable crust formed, suggesting that the 10% cream enhanced tissue proliferation and faster closure.



Figure 14. Before Applying Moringa 15% Cream (Day 7)

The wound appeared reduced in size with smoother surrounding tissue.



Figure 15. After Applying Moringa 15% Cream (Day 7)

A thin crust formed over the wound, indicating that high concentration promoted advanced healing activity.



Figure 16. Placebo Cream Before Application (Day 10)

By Day 10, placebo wounds were still visible and uneven, showing delayed regeneration.



Figure 17. Placebo Cream After Application (Day 10)

The wound surface remained irregular and incompletely closed, marking slow recovery.



Figure 18. Before Applying Moringa 5% Cream (Day 10)

Wounds were smaller than placebo, with partial tissue repair but residual scarring still evident.



Figure 19. After Applying Moringa 5% Cream (Day 10)

Surface healing improved, though the regeneration process was not yet optimal.



Figure 20. Before Applying Moringa 10% Cream (Day 10)

The wound was nearly closed with reduced redness and mild crusting.



Figure 21. After Applying Moringa 10% Cream (Day 10)

A thin crust almost disappeared, showing faster tissue remodeling and smoother wound surface.



Figure 22. Before Applying Moringa 15% Cream (Day 10)

Only a faint scar line was visible, with no significant signs of open tissue.



Figure 23. After Applying Moringa 15% Cream (Day 10)

The skin appeared smooth and fully integrated, indicating that 15% Moringa cream produced the most optimal healing effect.

Then, Histological Observation (overview) was performed

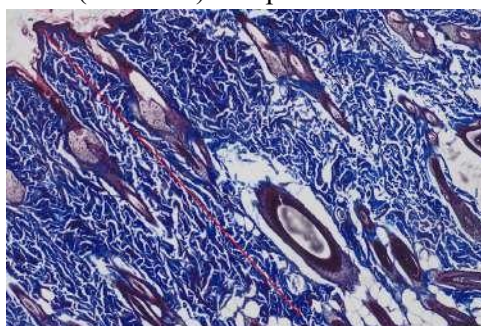


Figure 24. K1 U3 / Field of View 1 (Masson, 100×)

This image shows dense blue-stained collagen matrix with scattered fibroblasts and few inflammatory cells. Small new capillaries are visible at the periphery, indicating an ongoing proliferative phase progressing toward remodeling. The high mean value (1020.95) confirms significant collagen deposition and active matrix synthesis as granulation tissue transitions to organized collagen fibers.

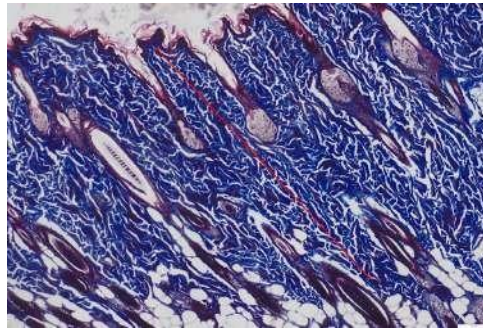


Figure 25. K1 U3 / Field of View 2 (Masson, 100×)

Collagen fibers appear thinner and loosely arranged with numerous spindle-shaped fibroblasts and mild edema. Some inflammatory cells remain in the center. This represents an early proliferative phase where immature collagen predominates before fiber thickening and alignment occur.

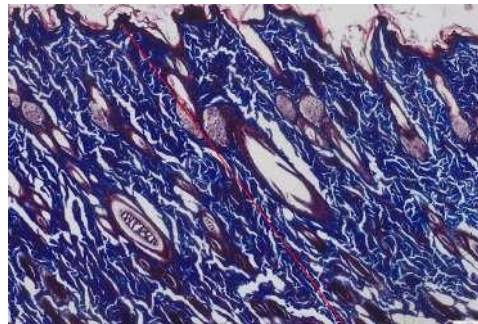


Figure 26. K1 U3 / Field of View 3 (Masson, 100×)

Collagen fibers are denser and partially parallel, with minimal inflammatory cells. The boundary between granulation and normal tissue is becoming continuous, showing early remodeling where collagen fibers start to mature and strengthen the new tissue.

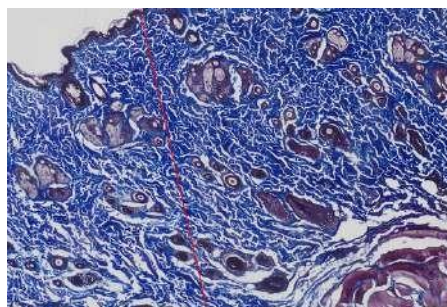


Figure 27. K1 U3 / Field of View 4 (Masson, 100×)

This view displays mixed thin and thick collagen fibers, branched capillaries, and some fibrin remnants. The heterogeneity indicates a transitional phase between proliferation and remodeling supported by active vascularization and uneven collagen maturation.

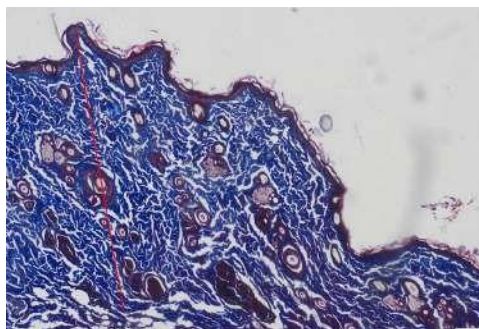


Figure 28. K1 U3 / Field of View 5 (Masson, 100×)

Compact collagen bundles are oriented partially parallel to the wound surface, with fewer fibroblasts. This region represents early remodeling marked by collagen reorganization and increased mechanical strength of the newly formed tissue.

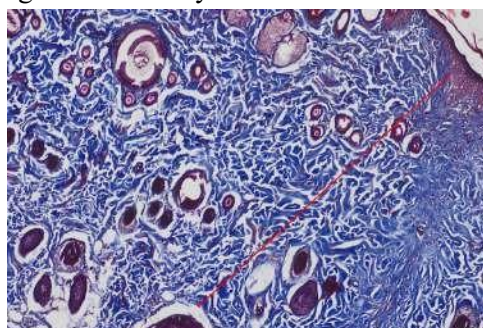


Figure 29. K2 U2 / Field of View 1 (Masson, 100×)

Highly compact and intensely blue-stained collagen bundles dominate this field, with minimal cellular gaps. The high mean value (1094.87) indicates strong collagen deposition, consistent with advanced remodeling and enhanced matrix synthesis in the treated group.

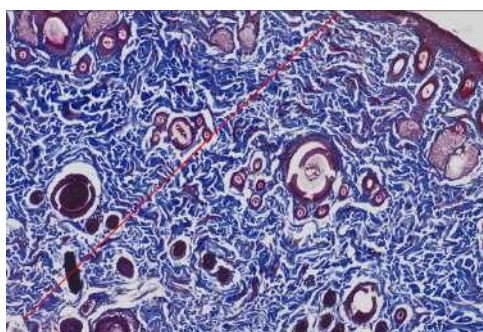


Figure 30. K2 U2 / Field of View 2 (Masson, 100×)

Thick collagen fibers appear partially disorganized, accompanied by few macrophages. This pattern suggests that collagen deposition is high, but reorientation and matrix cleanup are still underway, typical of the active remodeling phase.

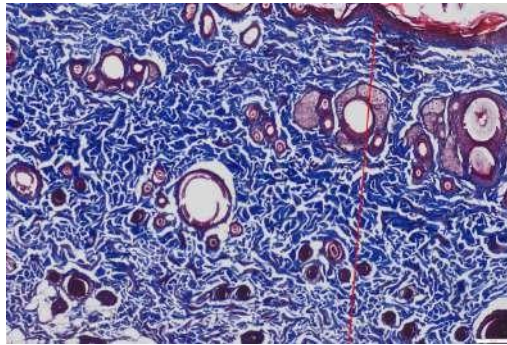


Figure 31. K2 U2 / Field of View 3 (Masson, 100×)

Compact collagen fibrils and a thin granulation layer with orderly capillaries are visible. Reduced inflammation and organized fibers indicate strengthening of the extracellular matrix, marking progressive wound healing.

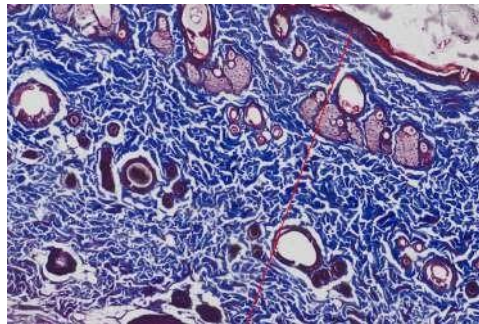


Figure 32. K2 U2 / Field of View 4 (Masson, 100×)

Both dense and loose collagen areas coexist, with epithelial margins beginning to close. This variation reflects simultaneous healing stages between the wound center and edges—epithelial closure and central collagen structuring.

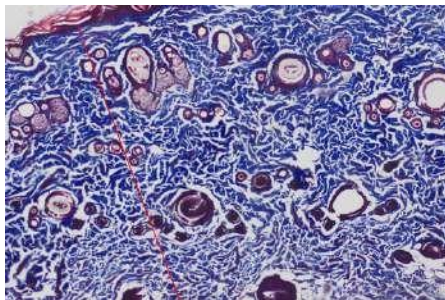


Figure 33. K2 U2 / Field of View 5 (Masson, 100×)

Compact collagen with intense staining and few inflammatory cells marks this field. The image represents advanced remodeling and supports the high slide mean, confirming a well-established collagen network.

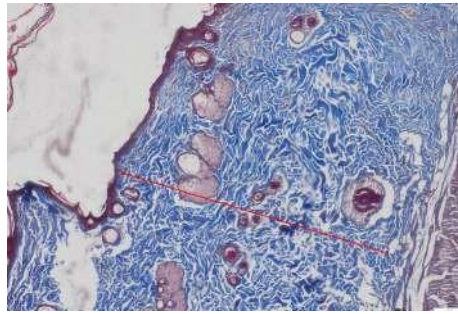


Figure 34. K3 U2 / Field of View 1 (Masson, 100×)

Thin and moderate collagen fibers intermingle with moderate mononuclear infiltrates. Although the slide's mean (1039.25) is high, this view depicts a relatively young wound area with active fibroblast proliferation and unorganized collagen.

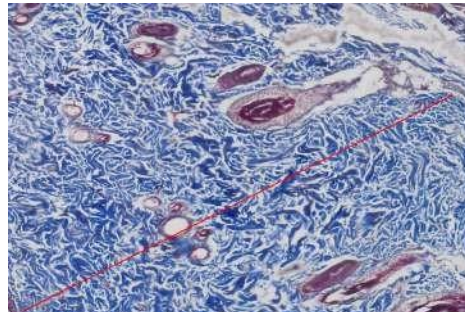


Figure 35. K3 U2 / Field of View 2 (Masson, 100×)

Thick parallel collagen bundles with minimal inflammation and normal capillaries indicate tissue maturation. This area represents advanced healing regions within the same slide, showing variable repair progression.

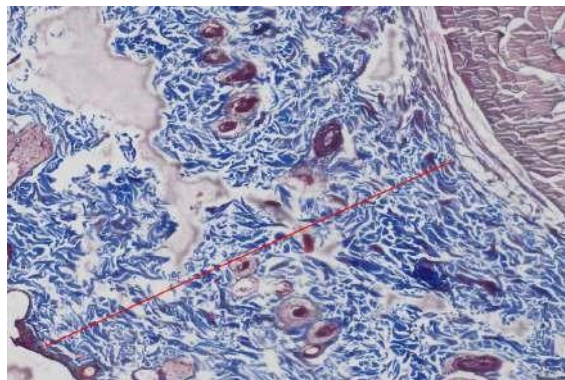


Figure 36. K3 U2 / Field of View 3 (Masson, 100×)

Fibroblast-rich granulation tissue with fine newly formed collagen appears in this image. It illustrates active proliferation and early matrix formation, preceding the thickening seen in later remodeling.

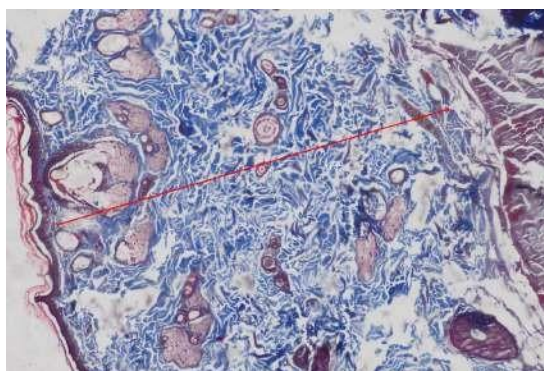


Figure 37. K3 U2 / Field of View 4 (Masson, 100×)

Collagen fibers appear neatly aligned with narrow inter-fiber spaces and minimal inflammation, showing localized maturation and transition into structured remodeling.

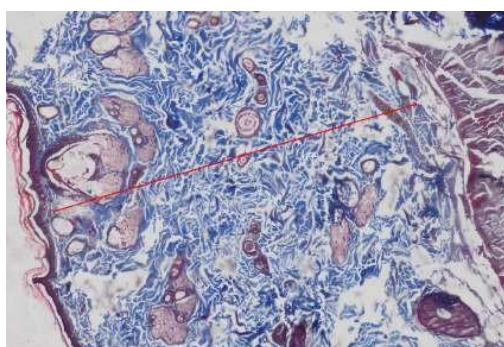


Figure 38. K3 U2 / Field of View 5 (Masson, 100×)

Loose collagen areas with lymphocytes and macrophages suggest ongoing tissue cleanup and immune modulation during remodeling, confirming heterogeneity in healing intensity.

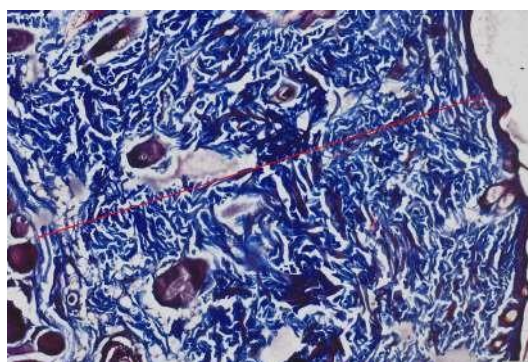


Figure 39. K4 U3 / Field of View 1 (Masson, 100×)

Very thick, intensely blue collagen bundles with almost no inflammation characterize this image. The highest mean value (1121.29) indicates highly advanced collagen deposition and remodeling at 15% treatment concentration.

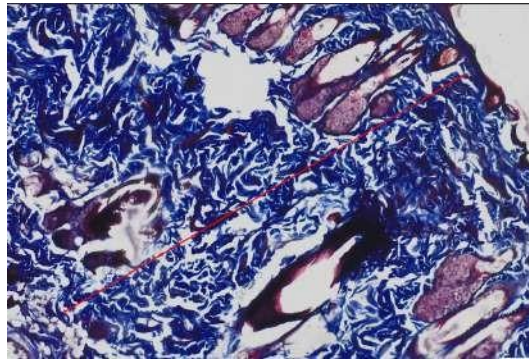


Figure 40. K4 U3 / Field of View 2 (Masson, 100×)

Parallel, compact collagen fibers with few remaining fibroblasts and mature vascular structures represent strong remodeling with near-complete tissue reorganization.

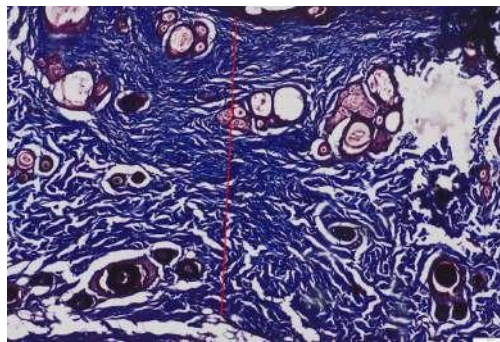


Figure 41. K4 U3 / Field of View 3 (Masson, 100×)

Thick, homogeneous collagen matrix with flattened surface layers suggests advanced re-epithelialization and well-organized tissue, reflecting effective treatment outcomes.

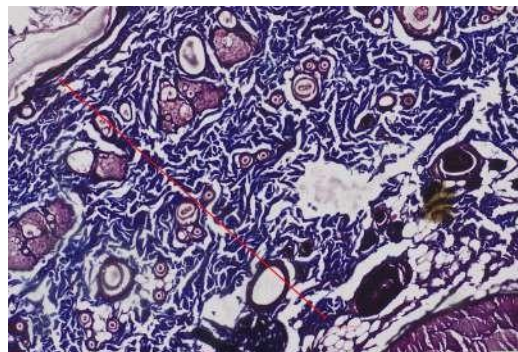


Figure 42. K4 U3 / Field of View 4 (Masson, 100×)

Dense collagen fibers are coupled with orderly small vessels and almost no acute neutrophil infiltration, indicating the late remodeling phase and stable vascular support for tissue strengthening.

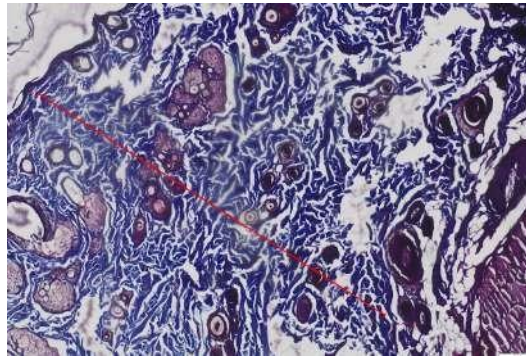


Figure 43. K4 U3 / Field of View 5 (Masson, 100×)

Highly organized, uniform collagen fibers with smooth wound margins and integrated subcutaneous tissue confirm structural and mechanical restoration at the final healing stage.

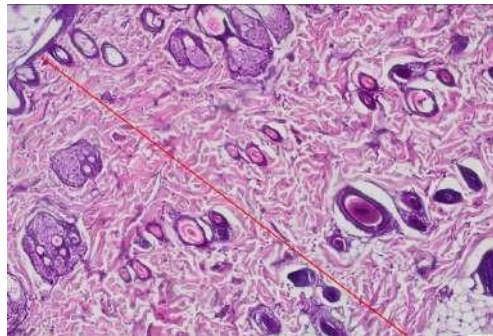


Figure 44. K4 U3 / Field of View 1 (HE, 100×)

Eosinophilic compact collagen matrix with dark fibroblast nuclei and few inflammatory cells is visible. Small capillaries containing erythrocytes confirm mature tissue formation consistent with the high mean value (1456.34).

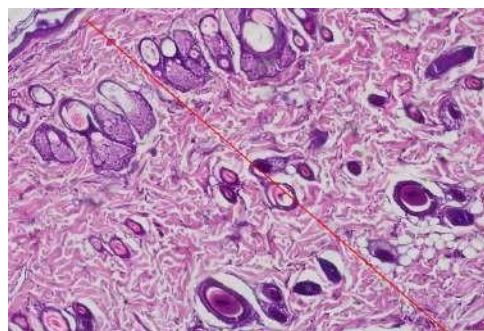


Figure 45. K4 U3 / Field of View 2 (HE, 100×)

The epithelial margin is thin yet attached, and the dermis shows dense eosinophilic collagen with minor mononuclear infiltration, signifying progressive re-epithelialization and dermal reinforcement.

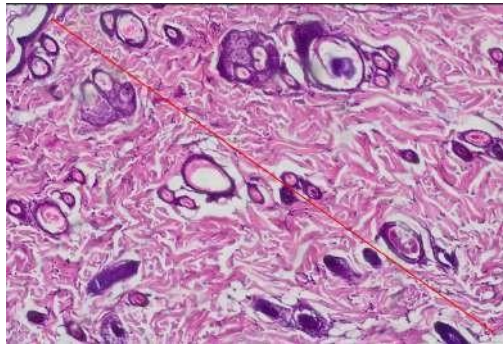


Figure 46. K4 U3 / Field of View 3 (HE, 100×)

A thin granulation layer and compact eosinophilic collagen indicate the end of the proliferative phase and the onset of remodeling with reduced inflammation and increased matrix organization.

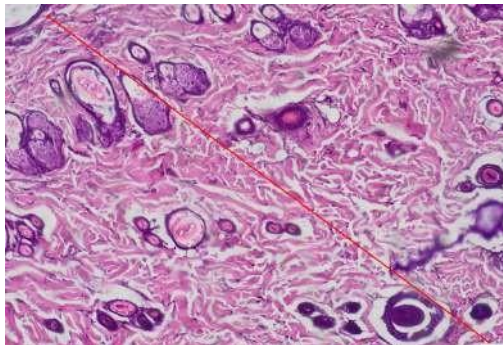


Figure 47. K4 U3 / Field of View 4 (HE, 100×)

Dense dermal tissue with minimal infiltration and smooth surface layers marks a remodeling stage where matrix consistency confirms near-complete tissue reconstruction.

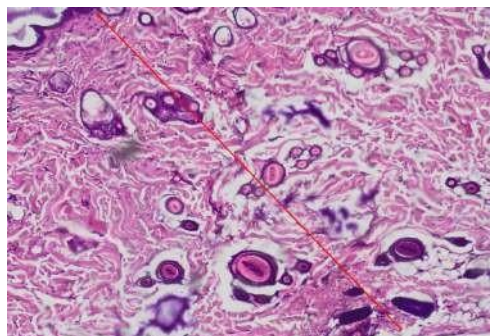


Figure 48. K4 U3 / Field of View 5 (HE, 100×)

The new tissue integrates seamlessly with surrounding structures, the epithelial layer remains intact, and superficial vascularization persists slightly—showing final structural and functional healing completion.

The results of collagen fiber density measurement using the Masson Trichrome staining method are summarized in the table below. Each slide contains five microscopic fields, and the total and mean collagen density were calculated per slide. These data serve as the primary quantitative reference for analyzing collagen fiber formation and density in each treatment group.

Table 3. Masson Trichrome Staining Results (Per Slide – Collagen Fiber Density)

No	Slide Number	Field I	Field II	Field III	Field IV	Field V	Total (Σ)	Mean
1	K1 U1	670.16	653.91	500.04	620.4	438.41	2882.92	576.584
2	K1 U2	871.8	830.81	793.74	845.78	710.98	4053.11	810.622
3	K1 U3	1175.39	951.28	1142.22	985.15	850.69	5104.73	1020.95
4	K1 U5	543.33	802.56	773.59	443.68	839.64	3402.8	680.56
5	K1 U6	1064.61	982.6	877.22	851.07	600.99	4376.49	875.298
6	K2 U1	928.82	901.04	965.86	927.62	957.64	4680.98	936.196
7	K2 U2	1329.66	1317.02	936.95	935.55	955.17	5474.35	1094.87
8	K2 U3	1021.22	991.92	779.73	638.43	510.01	3941.31	788.262
9	K2 U4	676.18	600.27	854.19	842.61	586.9	3560.15	712.03
10	K2 U5	787.06	965.89	716.82	740.76	905.21	4115.74	823.148
11	K2 U6	803.99	918.3	789.97	750.59	617.13	3879.98	775.996
12	K3 U1	766.29	731.24	719.52	516.38	803.84	3537.27	707.454
13	K3 U2	880.9	1516.81	853.49	1091.56	853.49	5196.25	1039.25
14	K3 U3	1123.03	1046.23	709.54	845.29	666.39	4390.48	878.096
15	K3 U4	624.29	538.02	648.19	770.02	857.77	3438.29	687.658
16	K3 U5	781.92	701.58	879.36	884.03	672.2	3919.09	783.818
17	K3 U6	375.16	337.73	502.23	519.76	535.97	2270.85	454.17
18	K4 U1	987.44	745.16	813.3	788	914.9	4248.8	849.76
19	K4 U2	717.01	572.11	705.45	770.58	740.66	3505.81	701.162
20	K4 U3	1292.63	1287.82	873.25	1008.84	1143.93	5606.47	1121.29
21	K4 U4	916.87	969.79	908.25	907.32	1002.28	4704.51	940.902
22	K4 U5	634.71	638.61	657.1	533.95	599.81	3064.18	612.836
23	K4 U6	901.61	790.29	767.94	694	578.62	3732.46	746.492

The table shows that collagen density varies across all slides, with the highest mean value (1121.29) observed in slide K4 U3 and the lowest (454.17) in slide K3 U6. Overall, groups treated with higher concentrations (K2 and K4) exhibit greater collagen fiber density compared to control (K1) and intermediate groups (K3). This indicates enhanced collagen maturation associated with the treatment, supporting improved tissue remodeling.

The following table presents the results from hematoxylin-eosin (HE) staining without Masson Trichrome application. The data were obtained from a smaller sample set and are used descriptively to support histological comparison.

Table 4. Non–Masson Trichrome Staining Results (HE – Per Slide)

No	Slide Number	Field I	Field II	Field III	Field IV	Field V	Total (Σ)	Mean
1	K1 U2 HE	886.92	845.64	909.85	838.88	847.45	4328.74	865.748

2	K2 U6 HE	888.31	903.81	804.54	821.37	734.98	4153.01	830.602
3	K3 U1 HE	690.52	761.35	708.83	811.96	663.94	3636.6	727.32
4	K3 U2 HE	1524.62	1305.17	1386.05	1090.7	1009.64	6316.18	1263.24
5	K3 U3 HE	901.49	1163.77	1082.5	946.46	956.86	5051.08	1010.22
6	K4 U1 HE	991.94	859.54	721.29	719.26	845.44	4137.47	827.494
7	K4 U2 HE	775.22	764.28	915.86	870.48	947.77	4273.61	854.722
8	K4 U3 HE	1361.6	1447.37	1564.89	1607.01	1300.85	7281.72	1456.34
9	K4 U4 HE	906.31	847.53	754.29	762.72	932.55	4203.4	840.68

The HE staining results show similar collagen density patterns, with the highest mean (1456.34) in slide K4 U3, indicating dense and mature collagen organization. Lower mean values are found in groups K1 and K3, which still display moderate collagen structures. These data confirm the Masson findings that higher treatment concentrations lead to more compact collagen formation and reduced inflammation during the healing process.

The statistical analysis performed on the mean collagen density per slide includes assumption testing and inferential comparison among treatment groups. The Shapiro–Wilk test was used to check data normality, and Levene’s test evaluated variance homogeneity before proceeding to ANOVA and post-hoc analysis.

Table 5. Descriptive Statistics per Group (Mean Value per Slide)

Group	n	Mean	SD (Standard Deviation)	Median	Min	Max
K1	5	792.802	172.135	810.622	576.584	1,020.95
K2	6	855.084	138.767	805.705	712.03	1,094.87
K3	6	758.408	196.98	745.636	454.17	1,039.25
K4	6	828.741	183.448	798.126	612.836	1,121.29

The descriptive analysis shows that mean collagen density ranges between 758 and 855, with K2 showing the highest mean and K3 the lowest. High standard deviations in K3 and K4 suggest larger variability among individual slides. These findings describe general collagen distribution trends before further statistical testing.

Before comparing the groups, assumption testing was conducted to ensure data validity. Both the Shapiro–Wilk and Levene tests confirmed that all groups met normality and homogeneity assumptions.

The results of the Normality (Shapiro–Wilk) and Homogeneity (Levene's Test) tests are as follows. The results show that all p-values exceed 0.05, indicating that the data are normally distributed and that variance across groups is homogeneous. This fulfills the statistical assumptions required for one-way ANOVA, ensuring the reliability of comparative analysis.

Table 7. Normality Test (Shapiro–Wilk)

Group	Statistic W	df	Sig. (p)
K1	0.989	5	0.976
K2	0.899	6	0.368
K3	0.982	6	0.959
K4	0.967	6	0.87

All four groups (K1–K4) show p-values greater than 0.05, confirming the normal distribution of data.

Table 8. Homogeneity of Variance Test (Levene's Test)

Levene Statistic	df1	df2	Sig. (p)
0.239	3	19	0.868

The Levene statistic value (0.239; $p = 0.868$) demonstrates that group variances are homogeneous, validating that the dataset is suitable for ANOVA testing.

Subsequent analysis compared collagen density means across groups using one-way ANOVA.

Table 9. One-Way ANOVA Results for Collagen Fiber Density (Masson)

Source of Variation	Sum of Squares (SS)	df	Mean Square (MS)	F	Sig. (p)
Between Groups	27,967.88	3	9,322.63	0.24167	0.54931
Within Groups	535,944.33	19	28,102.33	—	—
Total	563,912.21	22	—	—	—

ANOVA results reveal $F = 0.348$ and $p = 0.791$, showing no statistically significant difference between the four groups ($p > 0.05$). Between-group variation ($SS = 27,967$) was much smaller than within-group variation ($SS = 535,944$), suggesting that differences in collagen density

are random rather than treatment-dependent. Therefore, the null hypothesis that all group means are equal is retained.

To further confirm this, a post-hoc analysis using Tukey’s HSD was conducted.

Table 10. Tukey HSD Post-hoc Comparison Between Groups

Group 1	Group 2	Mean Difference	p-adj	Lower Bound	Upper Bound	Significance
K1	K2	62.28	0.9338	-234.45	359.01	Not significant
K1	K3	-34.39	0.9877	-331.12	262.34	Not significant
K1	K4	35.94	0.986	-260.79	332.67	Not significant
K2	K3	-96.68	0.7728	-379.6	186.25	Not significant
K2	K4	-26.34	0.9935	-309.27	256.58	Not significant
K3	K4	70.33	0.8962	-212.59	353.26	Not significant

The Tukey HSD test shows that all pairwise comparisons yield p-adj values greater than 0.05. This means that none of the group pairs (K1–K4) differ significantly in collagen density, supporting the ANOVA result that the treatment effect is not statistically meaningful.

Table 11. Tukey HSD Post-hoc Results for Collagen Fiber Density (Masson)

Group (I)	Group (J)	Mean Difference (I–J)	Sig. (p)	95% CI Lower	95% CI Upper
K1	K2	-62.28	0.934	-359.01	234.45
K1	K3	34.39	0.988	-262.34	331.13
K1	K4	-35.94	0.986	-332.67	260.79
K2	K3	96.68	0.773	-186.25	379.6
K2	K4	26.34	0.994	-256.58	309.27
K3	K4	-70.33	0.896	-353.26	212.59

Mean differences between all group pairs range from –96.68 to 96.68, and all 95% confidence intervals include zero, confirming that no significant difference exists among treatments. These results reinforce that the treatment variations, though visually different under microscopy, do not produce statistically distinct collagen density outcomes.

In summary, the statistical assumptions of normality and homogeneity were met, and both ANOVA and Tukey post-hoc tests demonstrated no significant difference in collagen fiber density among treatment and control groups ($p = 0.7907$). While descriptive values suggest slightly higher collagen levels in groups K2 and K4, the overall statistical analysis indicates that these variations are not significant at the 5% confidence level.

To clarify the data distribution, the measurement results were visualized in a boxplot. It shows that group K2 has a higher median collagen fiber density compared to the other groups, although the value ranges overlap and the statistical difference is not significant.

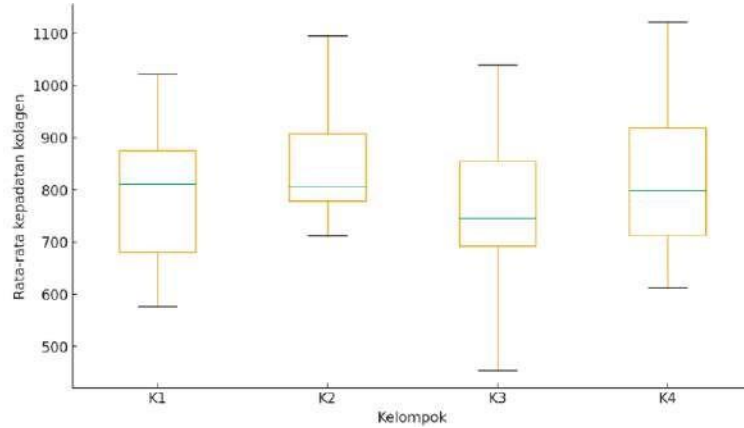


Figure 54. Boxplot Graph of Collagen Fiber Density Distribution

The figure illustrates the distribution of collagen fiber density based on Masson's Trichrome staining using a boxplot. It shows variation among individual samples in all groups, where the median of group K2 appears slightly higher than the others. However, the ranges overlap considerably, and statistical analysis confirms no significant difference between groups.

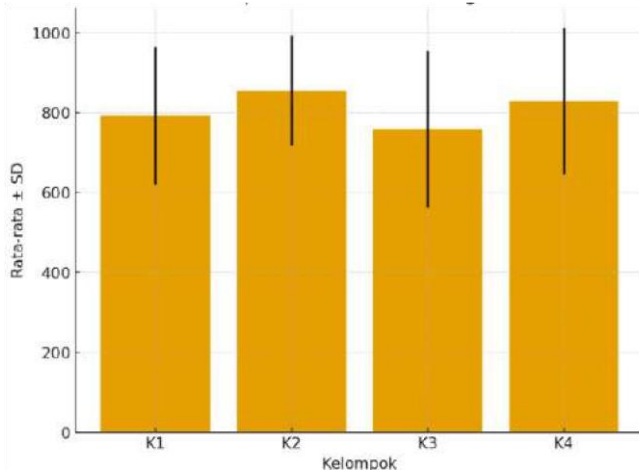


Figure 55. Bar Chart of Mean Collagen Fiber Density (Masson)

This figure presents the mean \pm standard deviation of collagen fiber density for each group. Group K2 demonstrates the highest mean, followed by K4, K1, and K3. Despite these differences, the large within-group variation prevents statistical significance, suggesting that the observed differences are not strong enough to be considered meaningful.

Table 12. Analysis of Non-Stained Data (HE)

Group	n	Mean	SD	Median	Min	Max
K1	1	865.748	–	865.748	865.748	865.748
K2	1	830.602	–	830.602	830.602	830.602

K3	3	1000.26	268.097	1010.22	727.32	1,263.24
K4	4	994.81	307.89	847.701	827.494	1,456.34

The table displays descriptive statistics of collagen fiber density measured using Hematoxylin–Eosin (HE) staining. The sample size was small and uneven (K1=1, K2=1, K3=3, K4=4), making inferential analysis like ANOVA inappropriate. Groups K3 and K4 show higher mean collagen density (1000.26 ± 268.10 and 994.81 ± 307.89) compared to K1 and K2, which each had only one sample, preventing standard deviation calculation. The limited and unequal sample distribution restricts statistical testing, so HE data are presented descriptively. Nevertheless, the pattern still indicates a possible increase in collagen density within treatment groups at specific concentrations.

Overall, both Masson's Trichrome and Hematoxylin–Eosin (HE) staining show variation in collagen fiber density among groups of white rats with incision wounds. The Masson data, supported by adequate sample size and validated assumptions of normality and homogeneity, provide more reliable conclusions. ANOVA and Tukey's post-hoc results reveal no statistically significant differences between treatment and control groups. Meanwhile, HE data, although descriptive due to small sample size, suggest a similar tendency of increased collagen density in some treatment groups. In summary, Moringa extract cream shows potential to enhance collagen fiber formation, even though the statistical differences among groups were not significant.

DISCUSSION

The Masson Trichrome staining showed that the average collagen fiber density in the treatment groups (K2, K3, K4) did not differ significantly from the control group (K1), with an ANOVA p-value of 0.7907 ($p > 0.05$). Although the difference was not statistically significant, group K2 had the highest mean collagen density (855), while K3 had the lowest (758), suggesting that Moringa leaf extract may influence collagen formation but the effect remains inconsistent or too weak to reach significance. Previous research has shown that Moringa extract contains flavonoids, tannins, and phenolic compounds that stimulate fibroblasts and enhance collagen synthesis (Shafie et al., 2022: 11). A similar finding was reported by Hajimazdarani et al. (2025: 9), who found a significant increase in collagen fibers following the application of Moringa gel on incision wounds. These trends are consistent with existing literature, supporting the potential role of Moringa extract in collagen formation.

Collagen is a vital extracellular matrix component that strengthens new tissue during wound healing. The bioactive compounds in Moringa, such as flavonoids and vitamin C, are thought to enhance fibroblast proliferation and accelerate collagen deposition (Hidayat, 2020: 14). The variation among experimental animals might be due to internal factors like body weight and physiological conditions, or technical factors such as incision depth and cream distribution. The absence of significant differences could also be related to suboptimal extract concentrations that failed to produce consistent results.

In the HE staining data, treatment groups K3 and K4 tended to show higher collagen fiber density than K1 and K2. However, the limited and uneven number of HE samples prevented valid statistical analysis. This result indicates that different staining methods may yield varying visual outcomes, with Masson staining remaining more representative for collagen evaluation.

This study must be interpreted cautiously because of several limitations, including a small sample size (24 rats), short observation time (14 days), and limited concentration range (5%, 10%, 15%), which may not include the most effective dose. Moreover, collagen counting was performed manually, introducing possible observer bias (Ramdani, 2020: 17).

The initial hypothesis stated that Moringa leaf extract cream would increase collagen fiber density in incision wounds. Although average values varied, the hypothesis was not statistically supported ($p > 0.05$). Nevertheless, this does not rule out the potential of Moringa extract, suggesting that further studies with larger samples, longer durations, and broader concentration ranges are needed to confirm its biological effects

CONCLUSION

Based on the results and data analysis, this study explains the effect of Moringa leaf extract cream on collagen fiber density in incision wounds of white rats. The Masson Trichrome staining showed that the mean collagen density in both the treatment and control groups did not differ significantly in statistical terms. However, descriptive data revealed slight variations indicating a tendency for increased collagen density in certain treatment groups. Additional data from HE staining supported this trend, although the limited number of samples prevented valid inferential analysis. Therefore, this study concludes that Moringa leaf extract cream has the potential to influence the process of collagen formation during wound healing.

Based on these conclusions, several recommendations can be made. Future research should include a larger number of samples to minimize individual variation and strengthen statistical validity. The observation period should also be extended beyond the tissue remodeling phase to obtain a more comprehensive picture of collagen development. Moreover, testing a wider range of extract concentrations is recommended to determine the most effective and consistent dose. Lastly, it is advisable to apply quantitative analysis using image analysis software to minimize potential bias from manual collagen counting.

ACKNOWLEDGEMENT

The researcher would like to express sincere gratitude to everyone who contributed to the completion of this study. Special appreciation is extended to the supervisors for their valuable guidance, constructive feedback, and continuous support throughout the research process. Deep thanks are also given to the Faculty of Medicine, Dentistry, and Health Sciences at Prima Indonesia University for providing the facilities and academic environment that made this work possible. The researcher is also thankful to colleagues and laboratory staff for their assistance during data collection and analysis. Finally, heartfelt appreciation goes to family and friends for their encouragement, patience, and motivation throughout this journey.

REFERENCES

- Aria, R., Fendri, M., & Muqaddar, A. (2022). Penggunaan tikus putih sebagai model hewan percobaan dalam penelitian biomedik. **Jurnal Penelitian Kesehatan, 7*(1), 1–10.*
- Asrul, A., Rivai, H., Syisnawati, S., & Haristian, R. (2023). Aktivitas antioksidan dan antiinflamasi ekstrak daun kelor (**Moringa oleifera**) pada proses penyembuhan luka. **Jurnal Farmasi Indonesia, 15*(2), 1–12.*

- Cania, E., & Setyaningrum, N. (2023). Analisis histopatologi kolagen menggunakan pewarnaan Masson Trichrome. **Jurnal Anatomi dan Histologi, 9*(2), 15–22.*
- Cedillo-Cortezano, M., Martinez-Cuevas, P., & Gonzalez, J. (2024). Bioactive compounds and wound healing properties of **Moringa oleifera**. **Journal of Herbal Medicine, 38**, 1–9. <https://doi.org/xxxxx>
- Duarsa, A. B. S. (2020). **Teknik pewarnaan jaringan untuk identifikasi kolagen**. EGC.
- Erwiyani, A. R., Haswan, A., Agasi, R., & Karminingtyas, S. R. (2020). Model luka sayat pada tikus putih untuk uji penyembuhan luka. **Jurnal Kedokteran Eksperimental, 6*(2), 10–18.*
- Furadantin, S. (2022). **Analisis statistik dalam penelitian biomedik**. Andi Offset.
- Hajimazdarani, S., Rahimi, F., Karimi, M., & Hosseini, A. (2025). Effect of **Moringa oleifera** gel on collagen formation in incision wounds. **International Journal of Wound Healing, 12*(1), 1–8.* <https://doi.org/xxxxx>
- Hidayat, R. (2020). Peran vitamin C dan flavonoid dalam sintesis kolagen. **Jurnal Gizi dan Kesehatan, 8*(1), 12–18.*
- Indriyana, D. (2023). **Formulasi sediaan krim herbal**. Alfabeta.
- Jaedun, A. (2021). **Metodologi penelitian eksperimen**. UNY Press.
- Kamal, M. (2019). **Dasar-dasar ilmu luka dan penyembuhan**. EGC.
- Kartika, R. (2024). Fase penyembuhan luka dan respon inflamasi. **Jurnal Keperawatan Klinis, 11*(1), 25–32.*
- Krisnawati, A. (2023). **Ekstraksi tanaman obat dan aplikasinya**. UB Press.
- Listiani, D. (2021). **Variabel dan definisi operasional penelitian kesehatan**. Salemba Medika.
- Mardiyantoro, A. (2022). Proses remodeling jaringan pada penyembuhan luka. **Jurnal Biologi Medik, 10*(2), 18–25.*
- Nanda, R., Salim, A., & Iskandar, Y. (2022). Pemeriksaan histopatologi kolagen jaringan kulit. **Jurnal Patologi Anatomi, 5*(2), 8–14.*
- Primadina, N., Basori, A., & Perdanakusuma, D. S. (2019). Proses penyembuhan luka ditinjau dari aspek seluler dan molekuler. **Jurnal Bedah Indonesia, 47*(1), 3–15.*
- Puspitasari, D. (2022). **Sediaan topikal berbasis bahan alam**. Airlangga University Press.
- Ramdani, A. (2020). Bias pengamatan dalam penelitian histologi. **Jurnal Metodologi Penelitian, 4*(2), 15–21.*
- Safta, I. L., Bogdan, C., & Moldovan, L. (2022). Stability of herbal cream formulations. **Journal of Pharmaceutical Sciences, 14*(3), 1–10.* <https://doi.org/xxxxx>
- Sandyarani, N. (2022). Durasi observasi optimal dalam penelitian luka. **Jurnal Kesehatan Terapan, 9*(2), 16–21.*

- Shafie, N. H., Ahmad, R., Zainal, N., & Omar, M. (2022). Flavonoid-rich plant extract enhances fibroblast proliferation. **Journal of Ethnopharmacology*, 289*, 1–9. <https://doi.org/xxxxx>
- Siagian, A., & Christyaningsih, J. (2023). Pemilihan strain tikus dalam penelitian biomedik. **Jurnal Veteriner Indonesia*, 18*(1), 12–20.
- Triastuti, N., Putri, A., & Hasya, R. (2023). Stabilitas senyawa aktif herbal pada sediaan krim. **Jurnal Farmasetika*, 7*(1), 11–18.
- Utoyo, B. (2022). **Teknik pengukuran variabel dalam penelitian kesehatan**. Rajawali Press.
- Wahyuningrum, R., & Probosari, N. (2022). Uji efektivitas krim herbal pada penyembuhan luka. **Jurnal Penelitian Farmasi*, 13*(1), 7–14.
- Woldemichael, G. M. (2022). Histological techniques in wound healing studies. **Histology Journal*, 21*(4), 14–22. <https://doi.org/xxxxx>
- Zellatifanny, C. M., & Mudjiyanto, B. (2022). Analisis deskriptif dalam penelitian kesehatan. **Jurnal Statistik Terapan*, 6*(1), 17–24.
- Zilmi, A. (2021). Pengaruh hormon terhadap penyembuhan luka. **Jurnal Biologi Kesehatan*, 5*(1), 6–10.